water

MDPI

Article

Impact of Exogenous Fulvic Acid Supplementation on Nitrogen Removal in a Single-Stage Partial Nitrification–Anammox (SNAP) Biofilm Reactor: Performance, Extracellular Polymeric Substances and Microbial Community

Chunli Yuan [1,*], Xinyue Ji [1], Changhao Lu [2,*] and Xin Xia [1]

[1] Key Laboratory of Regional Environment and Eco-Remediation, College of Environmental Engineering, Shenyang University, Shenyang 110044, China
[2] College of Mechanical Engineering, Shenyang University, Shenyang 110044, China
* Correspondence: chunlihappygirl@126.com (C.Y.); changhaolu@126.com (C.L.)

Abstract

Fulvic acid (FA) is the most redox-active fraction of humic substances in landfill leachate, and its effect on anammox has been studied mainly in anoxic biofilms. FA was added at 10, 50, 100 and 200 mg/L to a 4 L single-stage partial nitrification–anammox (SNAP) biofilm reactor fed with synthetic wastewater. The influent NH_4^+-N rose stepwise from 200 to 800 mg/L. The FA was oxygen-rich (O/C 0.64) and aliphatic. At the first step the influent strength doubled. The NH_4^+-N removal efficiency rose from 43.2% to 71.7%, reaching 87.6% at 100 mg/L. The nitrogen removal rate (NRR) increased from 0.30 to 0.69 kg N/(m^3·d) as the influent strength rose from 200 to 600 mg N/L. At 200 mg/L the removal efficiency and NRR fell to 53.0% and 0.40 kg N/(m^3·d). At 100 mg/L the polysaccharide, protein and humic substance contents of extracellular polymeric substances (EPS) rose from 4.78, 61.5 and 44.6 mg/g-VSS to 14.12, 147.4 and 161.3 mg/g-VSS. Nitrite reductase (Nir) and hydrazine dehydrogenase (Hdh) activities were 71.3% and 24.5% higher than in the control. *Candidatus Kuenenia* rose from 1.6% to 21.1% and *Denitratisoma* from 0.9% to 8.9%, while *Nitrosomonas* fell from 29.8% to 20.9%. The apparent optimum was 100 mg/L.

Keywords: single-stage nitrogen removal using anammox and partial nitrification (SNAP); fulvic acid; extracellular polymeric substances; enzyme activity; microbial community

1. Introduction

Anaerobic ammonium oxidation (anammox) converts NH_4^+ and NO_2^- to N_2 under autotrophic conditions and requires no external carbon source [1]. Because anammox bacteria (AnAOB) cannot produce NO_2^- themselves, the process is combined with partial nitrification, either in two separate reactors or in a single reactor. The single-stage process, termed single-stage nitrogen removal using anammox and partial nitrification (SNAP), was developed by Furukawa et al. [2] and has lower sludge production, no external carbon demand and lower operating costs than conventional nitrification–denitrification [3,4]. In a SNAP reactor, ammonia-oxidizing bacteria (AOB) and AnAOB are maintained in the same vessel, and stable operation depends on the balance between oxygen supply and oxygen consumption. Organic matter in the influent can disturb this balance and affect process performance.

Landfill leachate contains high concentrations of NH_4^+ and organic matter [5]. The organic fraction consists of readily degradable compounds and refractory humic substances,

Check for updates

Academic Editor: Cancan Jiang

Received: 2 November 2026
Revised: 16 November 2026
Accepted: 23 November 2026
Published: 27 November 2026

Copyright: © 2026 by the authors. Licensee MDPI, Basel, Switzerland. This article is an open access article distributed under the terms and conditions of the Creative Commons Attribution (CC BY) license.

the latter comprising humic acid (HA) and fulvic acid (FA) [6]. A SNAP reactor was used in our previous work to treat old landfill leachate [7], but the effect of the humic fraction was not examined separately. FA has a lower molecular weight and a higher oxygen content than HA and contains more quinone and phenolic groups, which give it a higher electron transfer capacity [8]. The effect of FA on SNAP therefore cannot be inferred from data obtained with HA.

Humic substances are conventionally divided into humic acid (HA), fulvic acid (FA) and humin according to their solubility, and the three fractions differ in molecular weight, oxygen content and functional-group composition. Humin is insoluble in both acid and alkali, has the highest molecular weight, and carries phenolic hydroxyl and amino groups whose electrons can be used by microorganisms for reductive respiration [9]. HA is soluble only above pH 2 and is more aromatic and less oxygenated than FA. FA has the lowest molecular weight of the three, is soluble at any pH, and is the most oxygen-rich fraction; its higher content of carboxyl, phenolic and quinone groups gives it the highest electron transfer capacity per unit mass, and in soil systems FA facilitates electron transfer more readily than HA [8]. These properties make FA the fraction most likely to act as a redox mediator, and its proportion among the humic substances of leachate changes as the landfill ages, so its contribution is the one most likely to shift during leachate treatment. HA and humin were not separated in this study, and this is stated as a limitation in Section 3.7.

Several studies have examined the effect of FA on anammox. Liu et al. [10] reported that short-term FA addition increased the release of N-acylated homoserine lactones (AHLs) and improved nitrogen removal. Zhang et al. [11] found that long-term addition of FA promoted sludge granulation and increased the nitrogen removal rate (NRR) when the influent total organic carbon (TOC) was 25.2–65.1 mg/L. At 15 °C, FA increased the expression of anammox functional genes and the levels of metabolites related to redox reactions and amino sugar metabolism [12]. Qiao et al. [13] compared mineral and biochemical FA in anammox granular sludge at 20 °C and reported NRR increases of 26.7% and 21.9% at 30 mg TOC/L. Li et al. [14] showed that HA and FA inhibited anammox-based systems above a threshold concentration and that the two fractions differed in the resistance they induced. In a 200-day moving-bed biofilm reactor, 50–100 mg/L FA increased the total nitrogen removal efficiency to 91%, whereas 200 mg/L caused dissimilatory nitrate reduction to ammonium (DNRA) and accumulation of NH_4^+ [15]. The response also depends on the molecular characteristics of the FA, as shown for denitrification with FA fractions of different aromaticity [16].

These studies were carried out with suspended, granular or biofilm anammox biomass without aeration, or with two-stage nitrification–anammox systems [10–15]. In a SNAP biofilm, aeration produces aerobic and anaerobic zones within the same biofilm, and AOB, AnAOB and heterotrophs compete for the same substrates, so FA may act differently from the anoxic systems described above. FA is a refractory humic fraction rather than a readily biodegradable substrate, and it is not treated as a carbon source in this study. Humic substances are essentially recalcitrant under anoxic conditions, and their microbial degradation requires oxygen or prior photolysis [17]; some aerobic and anaerobic bacteria can nevertheless degrade them slowly in soils and sediments [18]. A carbon-source contribution has been suggested for FA in anammox systems, so this possibility cannot be excluded a priori. The behavior reported for readily biodegradable carbon provides a point of comparison. In an anammox–denitrification system, nitrogen removal improved only up to a glucose concentration of 56.4 mg/L, and at 374.9 mg/L the NH_4^+-N removal efficiency fell from 97% to about 10% while the predominant genus shifted from *Ca. Kuenenia* to *Diaphorobacter* [19]. Heterotrophic denitrification consumes NO_2^- and NO_3^-, so an improvement driven by carbon supply is accompanied by a decrease in effluent NO_3^- and, above a threshold, by

the loss of the anammox population. Neither feature was observed here: effluent NO_3^--N did not decrease as the FA dose increased, and *Ca. Kuenenia* rose from 1.6% to 21.1%. The reported dose–response relationships are also difficult to compare, because the influent strength, temperature and biomass form differ among studies, and no upper dosage limit has been reported for a one-stage system. Where a mechanism has been proposed, it rests mainly on inferred rather than measured intermediates [10,12].

The objective of this study was to examine the effect of FA on nitrogen removal in a one-stage SNAP biofilm reactor. FA was added at 10, 50, 100 and 200 mg/L in a single reactor so that the concentrations could be compared under the same biomass history. The FA was characterized by scanning electron microscopy (SEM), elemental analysis, Fourier-transform infrared (FTIR) spectroscopy and X-ray photoelectron spectroscopy (XPS) to relate its structure to its electron transfer capacity. Reactor performance was evaluated together with EPS composition, the activities of five nitrogen-cycle enzymes and the microbial community, in order to identify the dosage range in which FA improves performance and the changes associated with the observed improvement.

2. Materials and Methods

2.1. Bioreactor

The reactor was an up-flow column of polymethyl methacrylate with an effective volume of 4 L, of the same design as that used in our previous work (Figure 1) [7]. A carrier (Teijin, Japan) was packed in the column so that biomass could attach and develop as a biofilm. The temperature was maintained at 32 °C by a heating rod. Dissolved oxygen (DO) was maintained at approximately 2.7 mg/L by aeration at the bottom of the column, and the pH was adjusted to 7.5–7.8 with $NaHCO_3$. A peristaltic pump fed the influent from the bottom and maintained the hydraulic retention time (HRT) at 12 h.

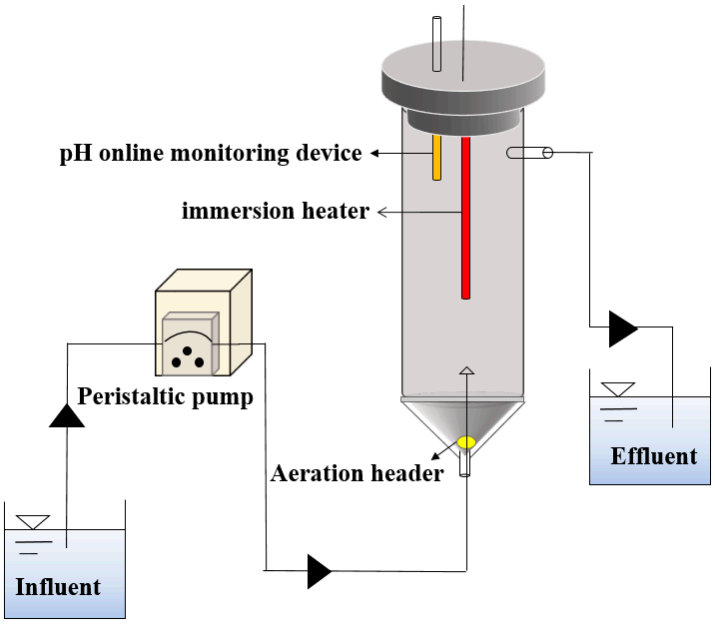


Figure 1. Schematic of the single-stage SNAP biofilm reactor.

2.2. Seeding Sludge

The biofilm was developed from sludge taken from a 2 m^3 SNAP reactor in our laboratory that had been operated for more than two years. The mixed liquor suspended solids (MLSS) and mixed liquor volatile suspended solids (MLVSS) of the seed sludge were approximately 12 and 10 g/L, respectively.

2.3. Synthetic Wastewater

A synthetic medium modified from van de Graaf et al. [20] was used. This medium is commonly applied for anammox enrichment because it provides the macro- and micronutrients required by AnAOB and contains no biodegradable organic carbon. $(NH_4)_2SO_4$ was the sole nitrogen source, KH_2PO_4 supplied phosphorus, and trace metals were provided by two stock solutions; the composition is given in Table 1. FA (Maya, jiaxing, Reagent, China) was dissolved in the influent to give concentrations of 0, 10, 50, 100 and 200 mg/L in the successive phases.

Table 1. Composition of the synthetic influent used in this study.

Component	Concentration
NH_4^+-N, as $(NH_4)_2SO_4$	200–800 mg/L
KH_2PO_4	68 mg/L
Trace element solution I [a]	0.5 mL/L
Trace element solution II [b]	0.1 mL/L
Mineral solution [c]	1 mL/L
Fulvic acid	0, 10, 50, 100, 200 mg/L

Notes: [a] EDTA 10 g/L, $FeSO_4$ 18 mg/L. [b] $NiCl_2{\cdot}6H_2O$ 1.9 mg/L, $MnCl_2{\cdot}4H_2O$ 9.9 mg/L, $ZnSO_4{\cdot}7H_2O$ 4.3 mg/L, $Na_2MoO_4{\cdot}2H_2O$ 2.2 mg/L, $CuSO_4{\cdot}5H_2O$ 12.5 mg/L, $CaCl_2{\cdot}6H_2O$ 12 mg/L, H_3BO_3 0.14 mg/L. [c] Modified from van de Graaf et al. [20].

Synthetic wastewater was used to avoid interference from the complex matrix of landfill leachate. Leachate contains biodegradable chemical oxygen demand (COD), variable alkalinity, inorganic ions and heavy metals, and its HA concentration changes with landfill age. These components would affect the response to FA and would prevent independent control of the FA concentration. With a defined medium, FA was the only variable among phases. Because the medium contained no biodegradable organic carbon, FA was also the only potential organic carbon source in the feed, which is relevant to the interpretation of the heterotrophic response in Section 3.5.1. The limitation of this approach is that the results describe the effect of FA in a defined medium rather than in a leachate matrix, as discussed in Section 3.7.

2.4. Reactor Start-Up and Operation

To establish the biofilm, 1 L of seed sludge and 3 L of deionized water were placed in the reactor and aerated for two days without feed. Synthetic wastewater was then introduced at an influent NH_4^+-N concentration of 200 mg/L. From day 7 onwards, the influent NH_4^+-N was increased by 100 mg/L whenever the effluent concentration fell below 50 mg/L. The reactor was monitored for 78 days, comprising a 32-day start-up period and a 46-day experimental period (days 32–78). During start-up, the influent strength was increased stepwise so that the biofilm could adapt to the applied load before FA was introduced.

A single reactor was operated. No replicate reactor was run, and all replicate measurements reported below are analytical replicates of samples taken from this reactor rather than independent biological replicates. In the experimental period, FA was added to the influent in four steps: 10 mg/L (Phase I), 50 mg/L (Phase II), 100 mg/L (Phase III) and 200 mg/L (Phase IV). Each concentration was maintained for 7–14 days, equivalent to 14–28 reactor turnovers. This is sufficient for the effluent composition to respond to a change in influent chemistry, but shorter than the doubling time of AnAOB. A step was considered complete when effluent NH_4^+-N, NO_2^--N and the NRR had varied by less than 10% over three consecutive days. The influent strength was increased in parallel, from 200 to 800 mg N/L, whenever effluent ammonium fell below the target value, so that the response to FA was examined at increasing load rather than at a single operating point. Performance under

each concentration is reported in Section 3.2, and the implications of the stepwise design for the interpretation of the biomass and enzyme data are discussed in Section 3.7.

2.5. Analytical Methods and Calculation of Performance Indices

MLSS, MLVSS and nitrogen species were determined according to Standard Methods [21]. The surface morphology of the FA powder was examined with a Hitachi SU8600 (Tokyo, Japan) scanning electron microscope (SEM), and the elemental composition was determined with a Elementar Analysensysteme GmbH elemental analyzer (Langenselbold, Germany). FTIR spectra were recorded on a Agilent Technologies Cary 630 FTIR spectrometer (Santa Clara, CA, USA) over 4000–500 cm^{-1} using KBr pellets. Surface elemental valence states were analyzed with a Thermo ESCALAB 250XI (Waltham, MA, USA) X-ray photoelectron spectrometer (XPS), and the C 1 s and O 1 s envelopes were deconvoluted for peak assignment.

The nitrogen removal rate was calculated as the mass of total nitrogen removed per unit effective reactor volume per unit time:

$$NRR = Q\,(C_{in} - C_{NH4,eff} - C_{NO2,eff} - C_{NO3,eff})/V \quad (1)$$

where NRR is expressed in kg N m^{-3} d^{-1}, Q is the influent flow rate (m^3 d^{-1}), C_{in} is the influent NH_4^+-N concentration and $C_{NH4,eff}$, $C_{NO2,eff}$ and $C_{NO3,eff}$ are the effluent concentrations of NH_4^+-N, NO_2^--N and NO_3^--N (kg N m^{-3}), and V is the effective reactor volume (m^3). The applied nitrogen load was calculated from the same equation with the effluent terms set to zero, and the NH_4^+-N removal efficiency as $(C_{in} - C_{NH4,eff})/C_{in}$. With V = 4 L and an HRT of 12 h, Q/V is 2 d^{-1}, so the applied load ranged from 0.40 kg N/(m^3·d) at 200 mg N/L to 1.60 kg N/(m^3·d) at 800 mg N/L.

The activities of nitrite reductase (Nir), hydrazine synthase (Hzs), hydrazine dehydrogenase (Hdh), nitrate reductase (Nar) and cytochrome *c* oxidase (Cox) were determined with sandwich enzyme-linked immunosorbent assays (ELISA) following the protocol of Hornbeck [22]. All samples were assayed with a single antibody lot on the same microplate, so inter-assay variability does not enter the comparisons reported here; three determinations were made per sample. ELISA quantifies immunoreactive protein rather than catalytic rate, so the absolute values should not be compared with those obtained by activity assays, and comparisons are made within this study only.

EPS were extracted from biofilm samples by thermal treatment at 60 °C for 30 min [13]. The extract was separated by centrifugation and filtered before analysis. Polysaccharide was determined by the phenol–sulfuric acid method with glucose as the standard. Protein and HS were determined by the Lowry method as described previously [23]: the extract was mixed with the alkaline copper reagent, the Folin–Ciocalteu reagent was added after incubation, and the absorbance was read against a calibration curve prepared with the corresponding standard. HS are not routinely included in the EPS fraction; they were included here because FA is itself a humic substance, and because HS showed the largest change among the EPS components (Section 3.3). The Lowry method responds to both protein and HS and is also subject to interference from other reducing compounds, and no correction was applied for this cross-reactivity. The protein values are therefore apparent concentrations that may include a contribution from HS, and because protein and HS increased together in this study, the two sets of values are not fully independent.

2.6. Microbial Community Analysis

The community structure was determined by 16S rRNA gene high-throughput sequencing (Majorbio, Shanghai, China). The V3–V4 region was amplified with the primers 338F (5′-ACTCCTACGGGAGGCAGCAG-3′) and 806R (5′-GGACTACHVGGGTWTCTAAT-3′)

under the following conditions: initial denaturation at 95 °C for 3 min; 27 cycles of 95 °C for 30 s, 55 °C for 30 s and 72 °C for 45 s; and a final extension at 72 °C for 10 min. The amplicons were examined by electrophoresis on a 2% agarose gel and purified with the AxyPrep DNA Gel Recovery Kit (AxyPrep Biosciences, Union City, CA, USA) [5]. The functional gene composition was predicted from the 16S profiles against the Clusters of Orthologous Groups (COG) database.

The sequencing gives relative abundances and was not accompanied by absolute quantification. No quantitative PCR, fluorescence in situ hybridization or AnAOB-specific activity assay was performed, so the abundances reported in Section 3.5 are proportions of the sequences obtained and not cell counts or biomass. Taxa present below the detection level of amplicon sequencing cannot be excluded, and the statement that a genus was the only one of its group detected refers to the genera recovered in these profiles.

2.7. Statistical Analysis

Replicate determinations were averaged, and the variability is reported as the standard deviation of the analytical replicates. The effect of FA concentration on the EPS fractions and on enzyme activities was tested by one-way analysis of variance (ANOVA), and the F statistics with their degrees of freedom are reported together with the corresponding p values; differences were considered significant at $p < 0.05$. Because a single reactor was operated, the ANOVA describes the analytical replicates and does not test differences between independent reactors. Nitrogen removal data are presented as phase averages together with the maximum and minimum of each phase.

3. Results and Discussion

3.1. Surface and Structural Characterization of the Fulvic Acid

The SEM images of FA are shown in Figure 2. At low magnification (Figure 2a,b), the surface was irregular and consisted of heterogeneously distributed particles. At higher magnification (Figure 2c,d), near-spherical particles with pores and adhering fine particles were observed. The surface area was not quantified.

The elemental composition of FA was C 41.39%, H 5.02%, O 35.22%, N 0.02% and S 4.79% by mass; the remaining 13.6% was attributed to ash and inorganic constituents. The atomic ratios were H/C 1.45, O/C 0.64, N/C 0.0004 and S/C 0.043. The low N/C ratio indicates a low degree of humification and a low nitrogen content. The H/C ratio of 1.45 indicates a mainly aliphatic structure with little aromatic condensation, which is typical of low-molecular-weight FA rather than of condensed humic acids [24]. The O/C ratio of 0.64 is high and indicates extensive oxygen substitution, that is, a high content of carboxyl, phenolic and quinone groups. These ratios indicate an oxygen-rich, nitrogen-poor and aliphatic FA. The quinone/phenol couple provides the electron-accepting and electron-donating capacity, and the low degree of condensation keeps these groups accessible [8,25].

The FTIR and XPS spectra are shown in Figure 3. In the FTIR spectrum (Figure 3a), the band at 1593 cm^{-1} was assigned to C=O stretching of quinones and conjugated ketones, and the band at 1211 cm^{-1} to C–O stretching of phenolic groups. The broad band at 3442 cm^{-1} was assigned to O–H stretching, and the bands at 1358, 1114 and 1036 cm^{-1} to C–O and C–O–C stretching of alcohols, ethers and polysaccharide-like structures. The strong oxygen-containing bands are consistent with the O/C ratio of 0.64. The XPS survey spectrum (Figure 3b) was dominated by C 1 s and O 1 s peaks at 285 and 531 eV. In the C 1 s spectrum (Figure 3c), 59.99% of the carbon was present as C–C/C=C, 33.74% as C–O–C and 6.27% as C=O. The O 1 s spectrum (Figure 3d) was fitted with two components at 532.43 and 531.67 eV, with relative areas of 68.72% and 31.28%. The coexistence of quinone-type C=O and phenolic C–O is consistent with the redox activity of FA [8].

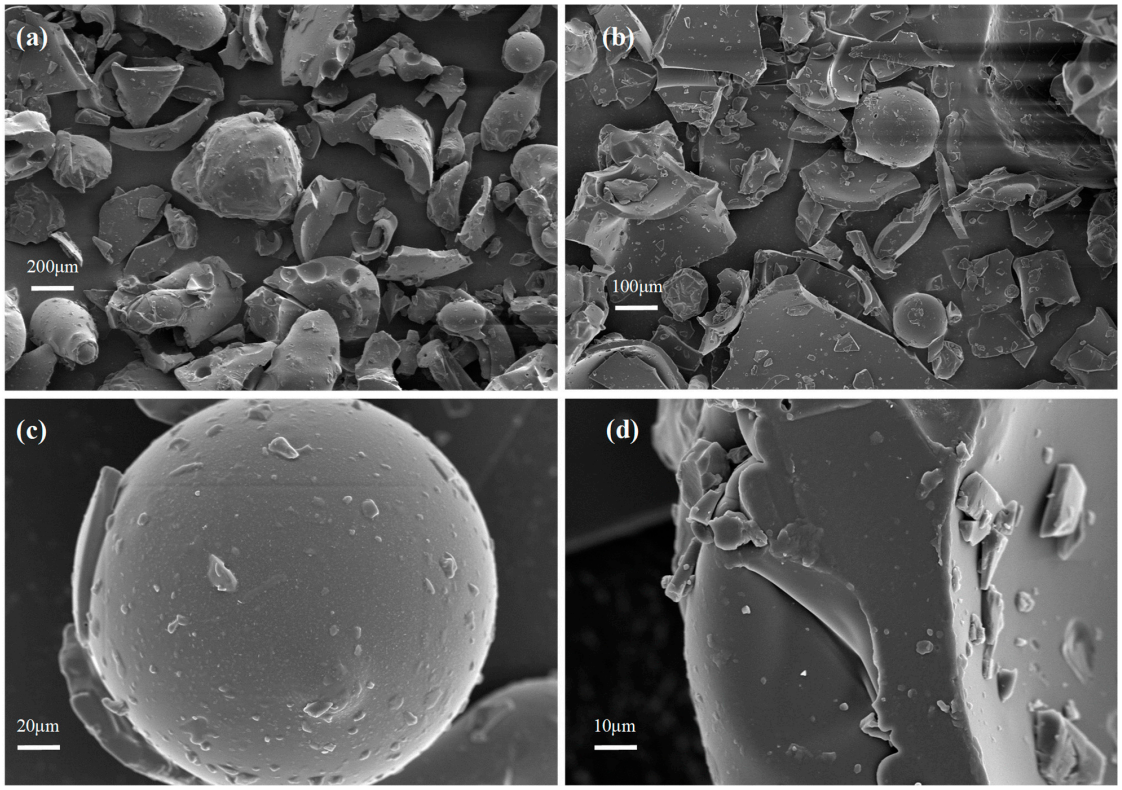


Figure 2. SEM images of the fulvic acid used in this study at (**a**,**b**) low and (**c**,**d**) high magnification. The scale bar of each panel is shown at the bottom of the micrograph.

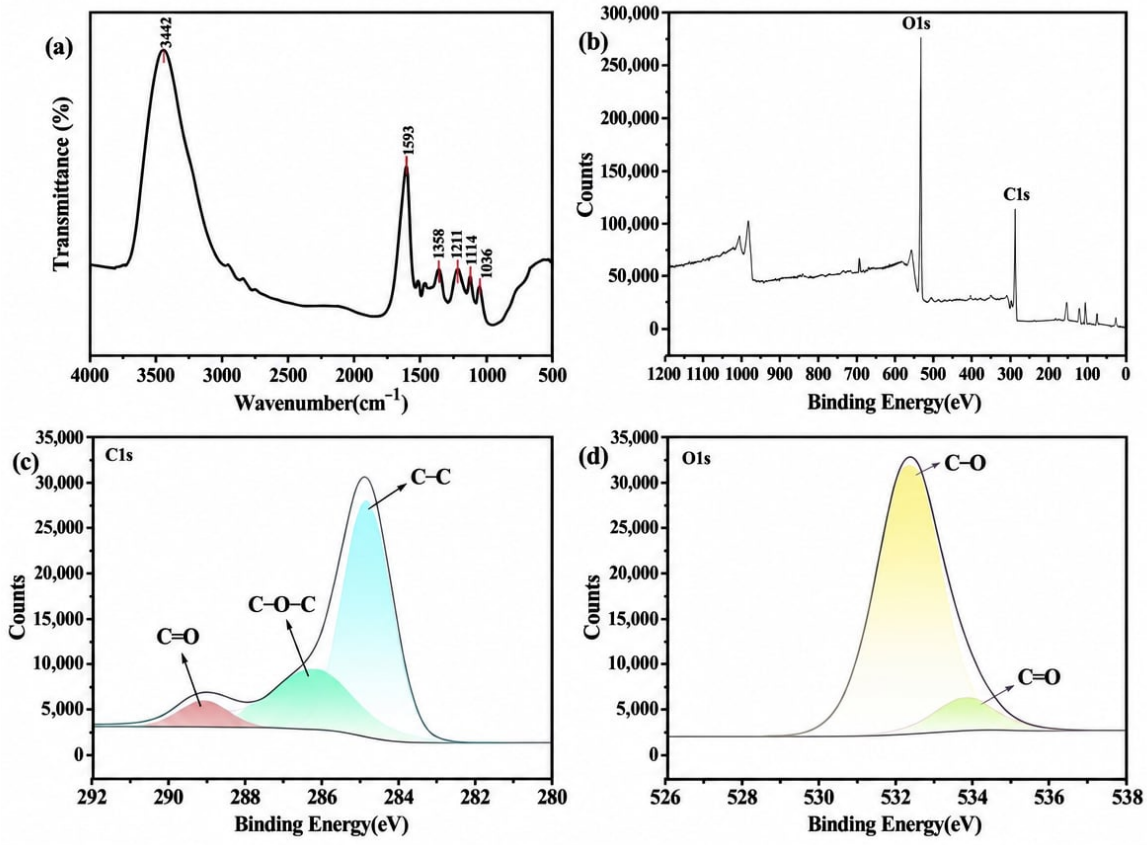


Figure 3. (**a**) FTIR spectrum of the FA; (**b**) XPS survey spectrum; (**c**) high-resolution C 1 s spectrum; (**d**) high-resolution O 1 s spectrum.

3.2. Nitrogen Removal Performance

The performance of the reactor before and after FA addition is shown in Figure 4. In Phase I (10 mg/L FA), the influent was raised from 200 to about 400 mg N/L. The NH_4^+-N removal efficiency increased from 43.2% to 71.7%, and effluent NH_4^+-N remained between 96 and 106 mg/L, with effluent NO_2^--N and NO_3^--N at about 4 and 48.6 mg/L. The NRR increased from 0.30 to about 0.55 kg N/(m^3·d) over this phase (Figure 4).

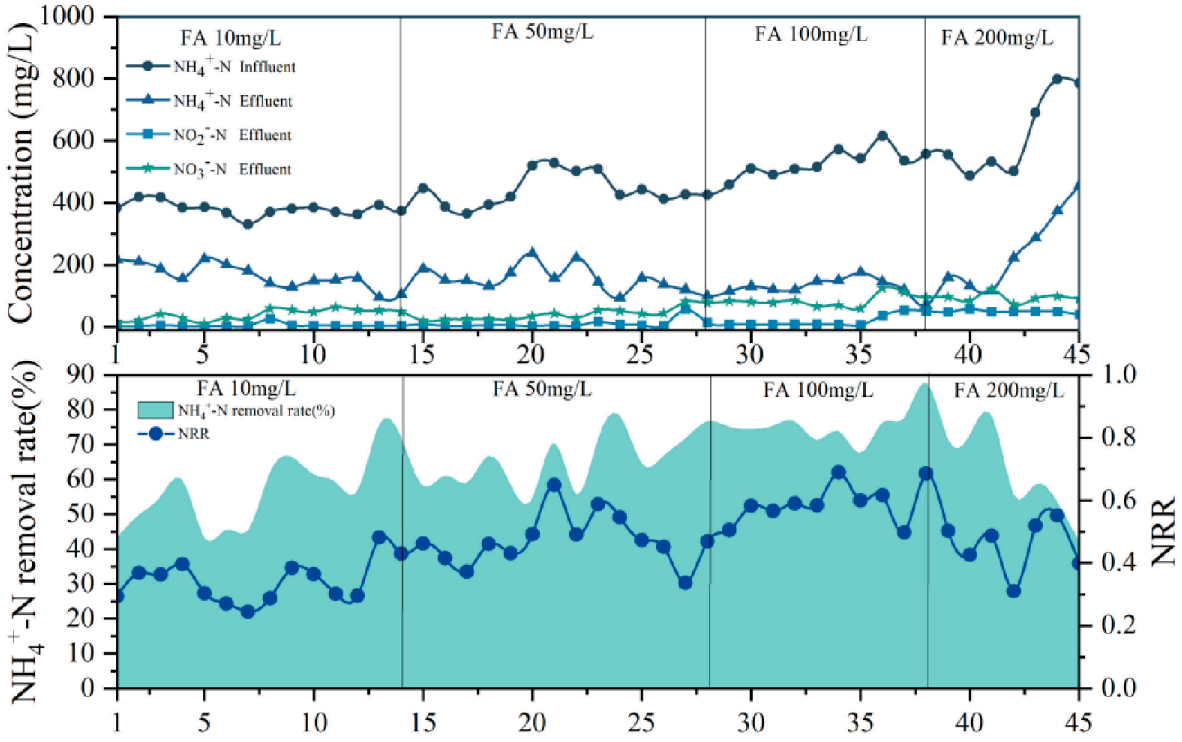


Figure 4. Influent and effluent concentrations of NH_4^+-N, NO_2^--N and NO_3^--N (upper) and NH_4^+-N removal efficiency and nitrogen removal rate (lower) during the experimental period. The FA concentration applied in each phase is indicated by the vertical lines. Values are measurements from the single reactor described in Section 2.4; no error bars are shown because no replicate reactor was operated.

In Phase II (50 mg/L FA), the influent was increased to 400 mg N/L after the FA concentration had been raised. The NH_4^+-N removal efficiency remained at about 70%, and effluent NO_2^--N and NO_3^--N were 14.2 and 77.3 mg/L. The NRR fluctuated between 0.35 and 0.62 kg N/(m^3·d) in this phase (Figure 4).

In Phase III (100 mg/L FA), the influent was raised to 600 mg N/L. The NH_4^+-N removal efficiency was 79–87.6%, with effluent NH_4^+-N between 49.8 and 99.7 mg/L, and effluent NO_2^--N and NO_3^--N were 51.4 and 94.4 mg/L. The NRR reached 0.69 kg N/(m^3·d), compared with 0.30 kg N/(m^3·d) before FA addition (Figure 4). After the 20% increase in influent strength the removal efficiency recovered within three days, which indicates that the biofilm was able to tolerate a further increase in load at this FA concentration.

In Phase IV (200 mg/L FA), the NH_4^+-N removal efficiency decreased below 70%, and effluent NO_2^--N and NO_3^--N were about 40 and 90 mg/L. When the influent was increased to about 800 mg N/L, effluent NH_4^+-N increased to 373.6 mg/L and the removal efficiency decreased to 53.0%. The NRR decreased to about 0.40 kg N/(m^3·d).

The influent strength was increased together with the FA concentration, so the increase in NRR from 0.30 to 0.69 kg N/(m^3·d) between the unamended period and Phase III (+130%) also includes the effect of the higher nitrogen load and is not an isolated measure

of the FA effect. The applied load rose from 0.40 to 1.60 kg N/(m^3·d) over the same interval (Section 2.5). The effect of FA can instead be read from the direction of change within each phase. In Phase I the NH_4^+-N removal efficiency increased by 28.5 percentage points while the influent was doubled, and in Phase III it recovered from 67.5% to 87.6% within three days of a 20% increase in influent strength. Both changes occurred against an increase in loading, which by itself would be expected to lower the removal efficiency. The percentage increases are also enlarged by the low removal efficiency of the unamended reactor (43.2%, 0.30 kg N/(m^3·d)), which was limited by incomplete nitrification rather than by the capacity of AnAOB.

Table 2 compares the results with those of previous studies on FA addition. The direction of the response is consistent with previous reports, in which FA at concentrations of tens of mg/L improved anammox performance in suspended, granular and biofilm systems [10–13]. The magnitude differs among studies. Qiao et al. [13] reported NRR increases of 26.7% and 21.9% at 30 mg TOC/L and 20 °C, and Cruz et al. [12] found that long-term FA addition at 15 °C improved performance mainly by alleviating low-temperature stress. In the present study, the low baseline NRR (0.30 kg N/(m^3·d)) resulted in a large percentage increase from a moderate absolute change; the 100 mg/L dose increased the NRR by 0.39 kg N/(m^3·d), and this value is more suitable for comparison with other systems than the percentage increase. The DO concentration of 2.7 mg/L in the SNAP reactor is a further difference, because the community was exposed to oxygen, which is not the case in the anoxic systems cited above.

Table 2. Comparison of the present results with previous studies on fulvic acid addition to anammox-based systems.

System and Biomass Form	FA Dose	Principal Response	Evidence Collected	Ref.
Suspended anammox, short-term exposure	FA, single dose	Nitrogen removal improved; AHL release increased	Performance, AHLs	[10]
Anammox granules, long-term	TOC 25.2–65.1 mg/L	Granulation promoted; NRR increased	Performance, community	[11]
Anammox biofilm, 15 °C, long-term	FA, continuous	Performance maintained at low temperature; expression of redox and amino sugar pathways increased	Metagenomics, metabolites	[12]
Anammox granules, 20 °C	30 mg TOC/L (mineral or biochemical FA)	NRR increased by 26.7% and 21.9%, respectively	EPS, electron transfer, community	[13]
Anammox moving-bed biofilm, 200 d	50–100 mg/L; 200 mg/L	TN removal up to 91%; at 200 mg/L DNRA occurred with NH_4^+ accumulation	Metagenomics, nitrogen flux	[15]
Two anammox-based systems	HA and FA, singly and combined	Inhibition thresholds identified; resistance differed between fractions	Performance	[14]
SNAP biofilm, 32 °C (this study)	10–200 mg/L	NH_4^+-N removal 43.2 → 87.6% while influent rose from 200 to 600 mg N/L; NRR 0.30 → 0.69 kg N/(m^3·d); performance decreased at 200 mg/L	Material chemistry, EPS, five enzymes, 16S community	This study

Notes: AHL, N-acylated homoserine lactone; DNRA, dissimilatory nitrate reduction to ammonium; HA, humic acid; NRR, nitrogen removal rate; TN, total nitrogen; TOC, total organic carbon.

The decrease in performance at 200 mg/L can be explained from the response of the nitrite-oxidizing bacteria (NOB). Effluent NO_3^--N remained at about 90 mg/L, close to its value at 100 mg/L FA, while NH_4^+-N accumulated. If AOB had simply been inhibited, the NO_2^- supply and therefore the production of NO_3^- would have fallen; the persistence of a high NO_3^- concentration instead indicates that NO_2^- continued to be oxidized. Under these conditions NOB compete with AnAOB for NO_2^-, the NO_2^- available to AnAOB decreases, and the NH_4^+ that AnAOB can no longer consume accumulates in the effluent. A contribution from DNRA cannot be excluded: Ye et al. [15] reported that 200 mg/L FA shifted the community of an anammox moving-bed biofilm towards DNRA and caused accumulation of NH_4^+, and such a shift would produce the same effluent pattern. Neither the *nrfA* gene nor an isotope tracer was measured here, and no closed nitrate balance was obtained, so DNRA remains a possibility rather than a demonstrated mechanism. Continued NOB activity requires no additional assumption, because NO_3^- was already accumulating at 100 mg/L and NOB were present in the biofilm. The influent was also increased to 800 mg N/L in this phase, and the effects of the two changes cannot be separated. What the data show is that 200 mg/L FA with 800 mg N/L exceeded the capacity of the biofilm, whereas 100 mg/L FA with 600 mg N/L did not. For this reactor configuration, 100 mg/L can therefore be regarded as the apparent upper limit of the useful dosage range under the conditions tested, and this value should be confirmed at the loading of a specific application.

3.3. Extracellular Polymeric Substances

The EPS composition at different FA concentrations is shown in Figure 5a. One-way ANOVA showed a significant effect of FA concentration on polysaccharide ($F(4,5) = 15.61$, $p = 0.005$), protein ($F(4,5) = 309.43$, $p < 0.001$) and HS ($F(4,5) = 914.90$, $p < 0.001$). The polysaccharide content increased from 4.78 mg/g-VSS in the control to 8.29, 10.32, 14.12 and 16.49 mg/g-VSS at 10, 50, 100 and 200 mg/L FA. The protein content increased from 61.5 to 147.4 mg/g-VSS at 100 mg/L (+140%) and decreased slightly to 144.5 mg/g-VSS at 200 mg/L. The HS content increased from 44.6 to 161.3 mg/g-VSS at 100 mg/L (+262%) and to 171.4 mg/g-VSS at 200 mg/L (+285%). The total EPS increased from 110.9 to 322.8 mg/g-VSS at 100 mg/L and to 332.5 mg/g-VSS at 200 mg/L. Protein was the only fraction that did not increase further at 200 mg/L, which coincided with the decrease in performance. Because the Lowry method responds to both protein and HS (Section 2.5), part of the apparent increase in protein may reflect the increase in HS, and the two values should not be treated as independent measures.

The increase in EPS, especially in HS, can be explained by three mechanisms. First, FA is a humic substance and contributes directly to the HS fraction of EPS through adsorption to the biofilm. Second, FA participates in intraspecies electron transfer, the tricarboxylic acid cycle and lipid biosynthesis and can therefore promote the synthesis of polysaccharide and protein [26]. Third, FA increases the release of AHLs such as C8-HSL and C12-HSL, which are known to induce EPS production [10,27]. The third mechanism is inferred from previous reports, because AHLs were not measured in this study.

The increase in EPS affects biofilm structure and reactor performance. The increase with FA concentration is consistent with previous observations in anammox biofilm systems [10]. Absolute EPS values differ among studies because of differences in extraction protocol, biomass characteristics and DO concentration; the thermal extraction used here recovers a relatively large fraction, and the inclusion of HS further increases the total, so the values should be compared within this study. The increase in polysaccharide and protein promotes aggregation and biofilm stability and improves biomass retention. Proteins in EPS can also act as extracellular enzymes that catalyze the conversion of NH_4^+-N and NO_2^--N [28]. The higher HS content increases the electron transfer capacity of the matrix [10,26].

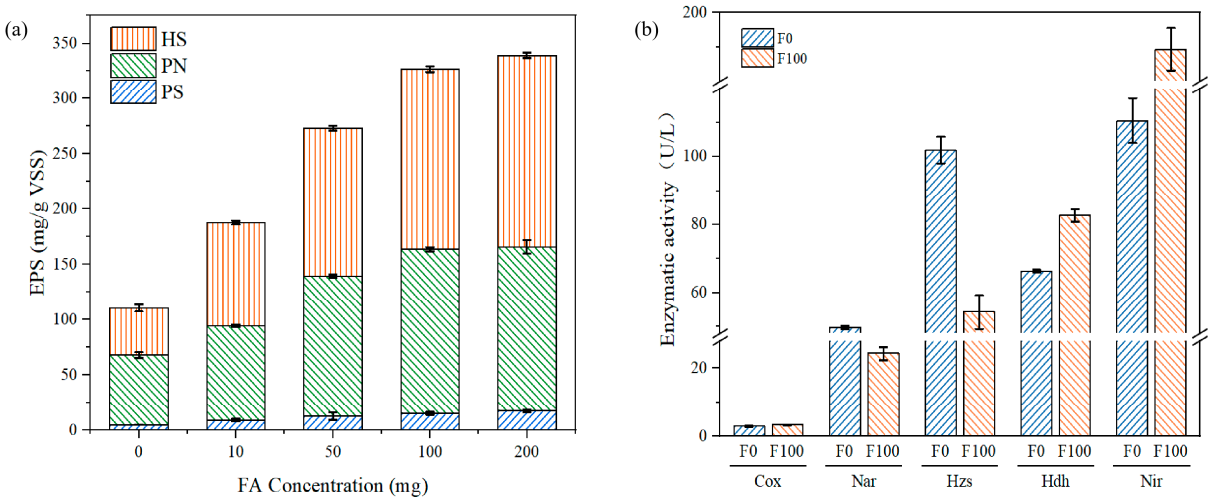


Figure 5. (**a**) Composition of extracellular polymeric substances and (**b**) activities of nitrogen-cycle enzymes in the biofilm at different FA concentrations. Values are means of three analytical replicates ($n = 3$) and error bars denote the standard deviation. In (**b**) only the control (F0) and the 100 mg/L treatment (F100) were assayed; the corresponding F and p values are given in Section 3.4.

3.4. Activities of Enzymes Involved in Partial Nitrification and Anammox

The activities of the five enzymes are shown in Figure 5b. The activities of Nir and Hdh reached maxima of 189.39 and 82.63 U/L at 100 mg/L FA, which were 71.3% and 24.5% higher than in the control. The activities of Nar and Hzs decreased by 51.3% and 46.7%, respectively. The difference between the control and the 100 mg/L treatment was significant for all four enzymes (one-way ANOVA, $F(1,4) = 169.8–479.3$, $p < 0.001$). Cox activity was low in both treatments and did not change appreciably. Nir and Hdh catalyze consecutive steps of the anammox pathway, and their activities determine the conversion of NO_2^- to N_2.

Two mechanisms may explain the increase in enzyme activity. FA can increase amino sugar metabolism and alter the intracellular amino acid pool [16], and amino acids such as glutamine, glutamic acid and glycine reduce protein hydrophobicity and increase conformational flexibility and catalytic efficiency [28]. In addition, AHL-mediated quorum sensing regulates enzyme expression in anammox consortia, so the increase in AHL release after FA addition may also increase enzyme activity [10,27]. The contribution of the two mechanisms cannot be separated with the present data, and the quorum-sensing route is inferred because AHLs were not measured.

The changes in individual enzyme activities are consistent with the nitrogen balance of the reactor. Nir reduces NO_2^- to NO [29], and Hdh oxidizes N_2H_4 to N_2 [30]; higher activities of both enzymes increase the conversion of NH_4^+ and NO_2^- to N_2. Nar reduces NO_2^- to NO_3^- and decreases total nitrogen removal, and its activity decreased, probably because Nir competed more effectively for NO_2^- [31]. Hzs activity also decreased, although performance improved. AOB can produce NO through incomplete nitrification, and AnAOB can use NO as an electron acceptor, so nitrogen removal can be maintained with low Hzs activity when the activities of Nir and Hdh are high [31]. Cox is related to electron transfer and ATP synthesis [26], but its activity did not change appreciably, so the electron transfer argument rests on the functional groups of FA rather than on the response of this enzyme. Enzyme activities were measured by ELISA, which determines immunoreactive protein rather than catalytic rate, so the absolute values should not be compared with those obtained by activity assays [22]; comparisons within this study are not affected because all samples were measured by the same procedure.

3.5. Microbial Community

3.5.1. Community Structure at the Genus Level

The microbial community at the genus level is shown in Figure 6a. *Candidatus* Kuenenia (*Ca. Kuenenia*) was the only anammox genus detected in the profiles. The two anammox genera most often recovered from wastewater reactors are *Ca. Kuenenia* and *Ca. Brocadia* [30], and only the former was found here, where it became the dominant anammox population. Its relative abundance increased from 1.6% without FA to 21.1% at 100 mg/L, and the two profiles followed a similar trend. The relative abundance is the proportion of the sequences obtained and not a measure of biomass, and genera present below the detection level of amplicon sequencing cannot be excluded. AHLs such as C6-HSL, C12-HSL and 3OC6-HSL can increase the growth rate of bacteria and affect community structure in anammox consortia [32,33].

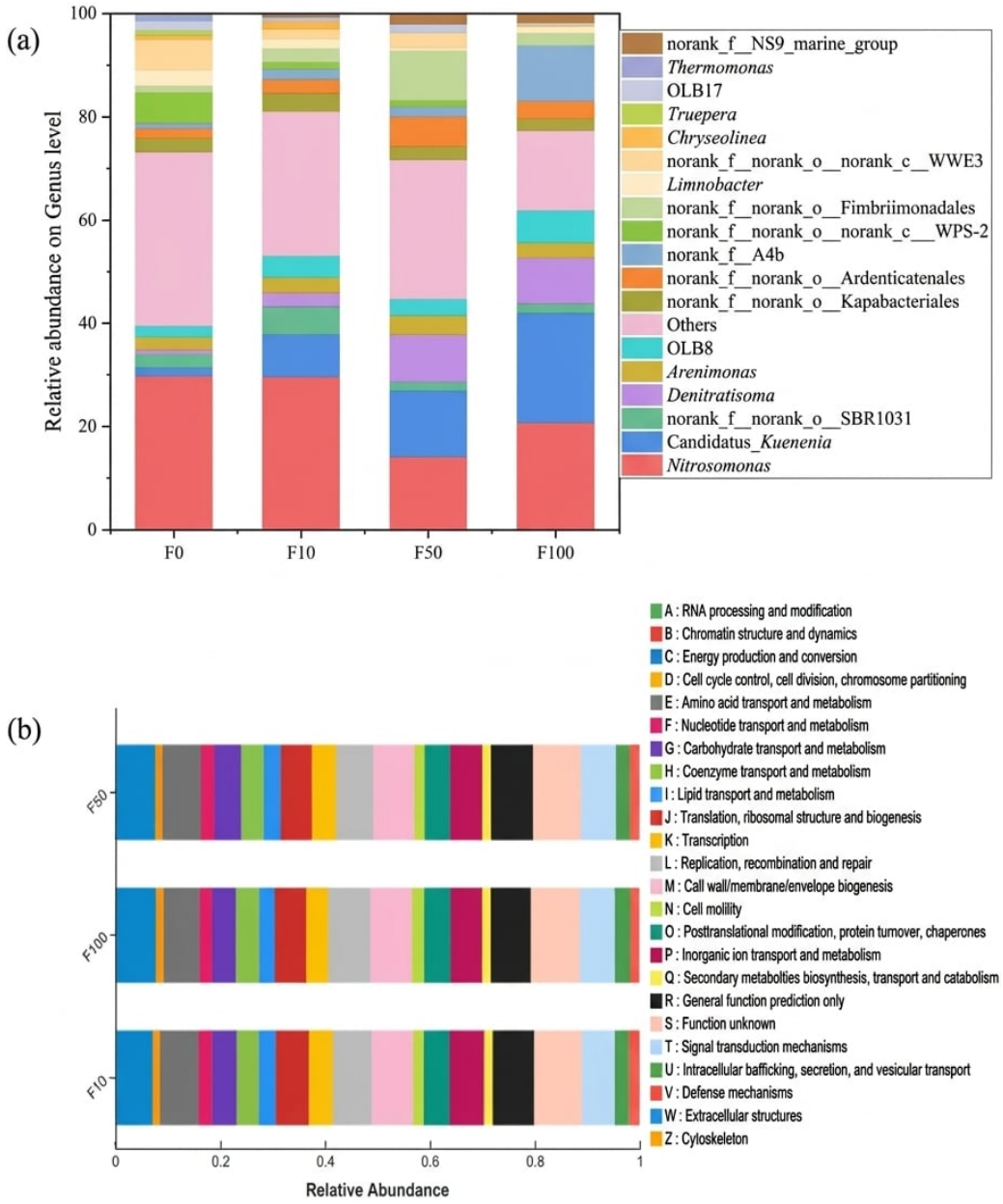


Figure 6. (**a**) Relative abundance of bacterial genera and (**b**) predicted functional gene composition at the COG level in the biofilm at different FA concentrations.

The relative abundance of *Nitrosomonas*, the main AOB genus, decreased from 29.8% in the control to 14.2% at 50 mg/L FA and then increased to 20.9% at 100 mg/L. Relative abundance reflects the proportion of a population in the community rather than its activity, so a decrease in the AOB fraction does not necessarily indicate a decrease in AOB activity. The increase in NRR indicates that AOB activity was maintained. The recovery at 100 mg/L may be related to competition for NO_2^-. The increase in *Ca. Kuenenia* would have increased the consumption of NO_2^- and decreased its concentration, which favors AOB with a higher substrate affinity [34,35].

Denitratisoma, a heterotrophic denitrifying genus that reduces NO_3^- to N_2 [36], increased from 0.9% in the control to 9.1% at 50 mg/L and 8.9% at 100 mg/L. An increase in this genus is consistent with a larger contribution from heterotrophic denitrification, which requires an organic substrate. The synthetic influent contained no biodegradable organic carbon, so the organic matter used by this genus must have come either from FA or from the EPS and soluble microbial products released by the biofilm, and the increase in EPS under FA addition provides a plausible substrate [37]. A general effect of carbon supply is not supported by the performance data. Where a readily degradable carbon source is supplied to an anammox system, heterotrophic denitrification consumes NO_2^- and NO_3^-, and above a threshold the anammox population is displaced [19]. At 100 mg/L FA the effluent NO_3^--N concentration remained high, at 94.4 mg/L, and *Ca. Kuenenia* increased, which is the opposite of that pattern. Utilization of FA itself was not measured and cannot be excluded. The growth of a nitrate-reducing population nevertheless provides a sink for part of the NO_3^- produced.

The changes in these three genera indicate that FA altered the composition of the community rather than stimulating a single population. The increase in *Ca. Kuenenia* and *Denitratisoma* is consistent with previous results [14]. The temporary decrease in *Nitrosomonas* at 50 mg/L and its recovery at 100 mg/L indicate that FA changed the competition among AOB, AnAOB and denitrifiers.

3.5.2. Predicted Functional Gene Composition

The predicted functional gene composition based on the COG database is shown in Figure 6b. The relative abundance of genes for energy production and conversion (category C) increased with FA concentration and reached about 7.0%, 7.6% and 7.7% in samples F10, F50 and F100, and that of genes for coenzyme transport and metabolism (category H) increased from 4.22% to 4.39%. The relative abundance of genes for translation, ribosomal structure and biogenesis (category J) decreased. These results suggest that FA increased the genetic potential for energy metabolism and decreased that for biomass synthesis.

Genes for lipid transport and metabolism (category I) were more abundant at 50 mg/L FA, as were genes for amino acid transport and metabolism (E), carbohydrate transport and metabolism (G) and general function prediction (R). An effect on membrane lipid metabolism is plausible given the phospholipid membrane of AnAOB and may improve resistance to environmental change, which is consistent with the performance at 50 mg/L. These categories were most abundant at 50 mg/L, whereas performance was highest at 100 mg/L, because COG profiles are predicted from taxonomic composition and describe genetic potential rather than gene expression.

3.6. Proposed Mechanism of Enhanced Reactor Performance

The proposed mechanism is based on the results of this study and on previous reports, and the steps that were not measured directly are indicated below. Two routes are considered: FA as a redox mediator, which is a hypothesis supported by the functional-

group composition of the FA, and FA as an organic carbon source, for which the measured responses provide no positive evidence but which cannot be excluded.

At the extracellular level, the increase in EPS, especially in protein and HS (Figure 5a), indicates a change in extracellular metabolism after FA addition. Part of this change may be related to quorum sensing. FA increases AHL release, and AHLs stimulate EPS synthesis and affect amino acid metabolism, which increases enzyme activity [10,27,28]. These processes may explain the increase in Nir and Hdh activities (Figure 5b). AHLs were not measured in this study, so this step is inferred from previous reports.

At the electrochemical level, the quinone and phenolic groups identified by FTIR and XPS (Figure 3) are of the kind that can act as a redox mediator, and FA may therefore facilitate extracellular electron transfer [8,26]. This is a hypothesis rather than a measured effect. No mediated electrochemical analysis, conductivity measurement or electron-transfer rate was determined in this study, and Cox activity did not change appreciably (Figure 5b). What the data support is that the FA added carries redox-active groups and that the community responded in a way consistent with improved energy metabolism, including the increase in *Ca*. *Kuenenia* (Figure 6a) [38,39]. The improvement cannot be attributed to electron transfer alone, because the simultaneous increase in *Denitratisoma* indicates that heterotrophic growth was also promoted.

At the community level, AOB supply NO_2^-, AnAOB consume it, and denitrifiers remove the NO_3^- produced by anammox, so the three groups are coupled [40]. Similar coupling between functional groups has been reported in single-stage anammox–denitrification reactors [41]. FA may therefore act through several routes at the same time. It relieves carbon limitation for heterotrophs, may increase electron transfer for AnAOB, and may affect EPS and enzyme synthesis through quorum sensing [8,26,27,39,40]. The AHL concentrations, the electron transfer rates and the fraction of FA carbon assimilated by the community were not measured, and these parts of the mechanism require further verification.

3.7. Limitations and Outlook

Seven limitations of this study should be noted. First, each FA concentration was maintained for 7–14 days, which is sufficient for the effluent to stabilize but shorter than the doubling time of AnAOB, so the biomass composition and the community and enzyme data may not represent a steady state at each concentration. Second, the concentrations were applied in increasing order in a single reactor, so the effects of concentration and time cannot be separated. Third, the reactor was not replicated, which is common for biofilm experiments of this duration but limits statistical inference for the performance data; the ANOVA in Section 2.7 applies to analytical replicates. Fourth, synthetic wastewater was used, so the results describe the effect of FA in a defined medium and do not include the interaction of FA with the biodegradable COD, HA and inorganic components of leachate, where competition between heterotrophs and AnAOB for oxygen and substrate would be stronger.

Fifth, neither the biodegradability of FA nor its contribution to the carbon balance was measured, and no carbon-source control was included, so the carbon-source and redox-mediator roles of FA cannot be separated with these data. Sixth, the explanation offered for the loss of performance at 200 mg/L is indirect: the *nrfA* gene, isotope tracers and a closed nitrate balance were not determined, and the concurrent increase in influent strength to 800 mg N/L cannot be separated from the increase in FA concentration. The transition between the effective and the inhibitory concentration was not resolved either, because a dose between 100 and 200 mg/L, for example 150 mg/L, was not tested. Seventh, HA and humin were not separated from FA, although all three fractions can participate in microbial

redox reactions, so the results describe the effect of the FA fraction alone and not that of the humic substances as a whole.

Further work should include a long-term experiment at a fixed FA concentration with replicate reactors and an unamended control, to determine whether the optimum at 100 mg/L is maintained and whether the change in community persists. A dose between 100 and 200 mg/L would locate the transition between the effective and the inhibitory range. Measurements of AHLs, electron transfer capacity, FA biodegradability and metagenomic or metatranscriptomic profiles would allow the proposed mechanism to be tested directly, and isotope tracing or quantification of *nrfA* would establish whether DNRA contributes at high FA concentrations. The dosage range should also be examined with real leachate of different landfill ages, in which the FA/HA ratio and the biodegradable fraction vary.

4. Conclusions

FA improved nitrogen removal in a single-stage SNAP biofilm reactor within a limited concentration range. At 10–100 mg/L the NH_4^+-N removal efficiency increased from 43.2% to 87.6% while the influent strength rose from 200 to 600 mg N/L, and the highest NRR, 0.69 kg N/(m^3·d), occurred at 100 mg/L. At 200 mg/L the removal efficiency decreased to 53.0%. The improvement was accompanied by higher EPS, Nir and Hdh activities and a higher relative abundance of *Ca. Kuenenia* and *Denitratisoma*. Because load and dosage increased together in a single reactor, the carbon-source and redox-mediator roles of FA remain to be separated.

Author Contributions: Conceptualization, C.Y. and C.L.; methodology, C.Y., X.J. and C.L.; validation, C.Y.; investigation, C.Y. and X.X.; data curation, C.Y. and X.X.; writing—original draft preparation, C.Y.; writing—review and editing, C.Y., X.J. and C.L.; project administration, C.L.; funding acquisition, C.Y. All authors have read and agreed to the published version of the manuscript.

Funding: This research was supported by the Young Scientists Fund of the National Natural Science Foundation of China (grant number 42507347), the Doctoral Start-up Foundation of Liaoning Province (grant number 2025-BS-0880) and the Basic Scientific Research Fund of the Education Department of Liaoning Province (grant number LJ212511035004).

Data Availability Statement: The original contributions presented in this study are included in the article. Further inquiries can be directed to the corresponding authors.

Conflicts of Interest: The authors declare no conflicts of interest.

References

1. Li, J.; Li, J.; Gao, R.; Wang, M.; Yang, L.; Wang, X.; Zhang, L.; Peng, Y. A critical review of one-stage anammox processes for treating industrial wastewater: Optimization strategies based on key functional microorganisms. *Bioresour. Technol.* **2018**, *265*, 498–505. [CrossRef]
2. Furukawa, K.; Lieu, P.K.; Tokitoh, H.; Fujii, T. Development of single-stage nitrogen removal using anammox and partial nitritation (SNAP) and its treatment performances. *Water Sci. Technol.* **2006**, *53*, 83–90. [CrossRef]
3. Fux, C.; Boehler, M.; Huber, P.; Brunner, I.; Siegrist, H. Biological treatment of ammonium-rich wastewater by partial nitritation and subsequent anaerobic ammonium oxidation (anammox) in a pilot plant. *J. Biotechnol.* **2002**, *99*, 295–306. [CrossRef]
4. Uyanik, S.; Bekmezci, O.K.; Yurtsever, A. Strategies for successful ANAMMOX enrichment at laboratory scale. *Clean Soil Air Water* **2011**, *39*, 653–657. [CrossRef]
5. Liu, J.; Zhang, H.; Zhang, P.; Wu, Y.; Gou, X.; Song, Y.; Tian, Z.; Zeng, G. Two-stage anoxic/oxic combined membrane bioreactor system for landfill leachate treatment: Pollutant removal performances and microbial community. *Bioresour. Technol.* **2017**, *243*, 738–746. [CrossRef]
6. Chardi, K.J.; Schenkeveld, W.D.C.; Kumar, N.; Giammar, D.E.; Kraemer, S.M. Effect of competing metals and humic substances on uranium mobilization from noncrystalline U(IV) induced by anthropogenic and biogenic ligands. *Environ. Sci. Technol.* **2023**, *57*, 16006–16015. [CrossRef]

7. Yuan, C.; Lu, C.; Ma, Y.; Wang, Y.; Xie, Y.; Zhang, K.; Wang, Y.; Lv, L.; Feng, X.; Zhu, T. A novel method to treat old landfill leachate combining multi-stage biological contact oxidation (MBCO) and single-stage autotrophic nitrogen removal using anammox and partial nitrification (SNAP). *Chem. Eng. J.* **2019**, *359*, 1635–1643. [CrossRef]
8. Yang, S.; Wang, K.; Yu, X.; Xu, Y.; Ye, H.; Bai, M.; Zhao, L.; Sun, Y.; Li, X.; Li, Y. Fulvic acid more facilitated the soil electron transfer than humic acid. *J. Hazard. Mater.* **2024**, *469*, 134080. [CrossRef]
9. Zhang, Z.; Liu, X.; Li, Z.; Chen, X.; Zu, Y.; Ho, S.-H.; Liang, B.; Zhou, S.; Wang, A. Humin oxidation drives microbial dehalogenation in oligotrophic environments. *ISME J.* **2025**, *19*, wraf207. [CrossRef]
10. Liu, L.; Ji, M.; Wang, F.; Tian, Z.; Wang, T.; Wang, S.; Wang, S.; Yan, Z. Insight into the short-term effect of fulvic acid on nitrogen removal performance and N-acylated-L-homoserine lactones (AHLs) release in the anammox system. *Sci. Total Environ.* **2020**, *704*, 135285. [CrossRef]
11. Zhang, L.; Wang, Y.; Soda, S.; He, X.; Hao, S.; You, Y.; Peng, Y. Effect of fulvic acid on bioreactor performance and on microbial populations within the anammox process. *Bioresour. Technol.* **2020**, *318*, 124094. [CrossRef]
12. Liu, L.; Wang, F.; Xu, S.; Yan, Z.; Ji, M. Long-term effect of fulvic acid amendment on the anammox biofilm system at 15 °C: Performance, microbial community and metagenomics analysis. *Bioresour. Technol.* **2022**, *344*, 126234. [CrossRef]
13. Qiao, L.; Feng, Y.; Liu, S.; Yan, P. Enhancing nitrogen removal efficiency for anammox granular sludge at low temperature by fulvic acids from different sources. *J. Water Process Eng.* **2024**, *60*, 105178. [CrossRef]
14. Li, X.; Du, R.; Zhang, J.; Peng, Y. Individual and combined effect of humic acid and fulvic acid on distinct anammox-based systems: Inhibition and resistance. *Chem. Eng. J.* **2022**, *444*, 136547. [CrossRef]
15. Ye, Y.; Miao, H.; Fang, W.; Ni, J.; Yang, K.; Gu, P.; Ren, X.; Zhang, Z. Deciphering dual effects of humic substrates on anaerobic ammonium oxidation: From metabolic facilitation to systemic nitrogen flux interference. *Bioresour. Technol.* **2026**, *455*, 134791. [CrossRef]
16. Li, M.; Chen, Y.; Su, Y.; Wan, R.; Zheng, X. Effect of fulvic acids with different characteristics on biological denitrification. *RSC Adv.* **2016**, *6*, 14993–15001. [CrossRef]
17. Coates, J.D.; Cole, K.A.; Chakraborty, R.; O'Connor, S.M.; Achenbach, L.A. Diversity and ubiquity of bacteria capable of utilizing humic substances as electron donors for anaerobic respiration. *Appl. Environ. Microbiol.* **2002**, *68*, 2445–2452. [CrossRef]
18. Park, H.J.; Kim, D. Isolation and characterization of humic substances-degrading bacteria from the subarctic Alaska grasslands. *J. Basic Microbiol.* **2015**, *55*, 54–61. [CrossRef]
19. Qin, Y.; Cao, Y.; Ren, J.; Wang, T.; Han, B. Effect of glucose on nitrogen removal and microbial community in anammox-denitrification system. *Bioresour. Technol.* **2017**, *244*, 33–39. [CrossRef]
20. van de Graaf, A.A.; de Bruijn, P.; Robertson, L.A.; Jetten, M.S.M.; Kuenen, J.G. Autotrophic growth of anaerobic ammonium-oxidizing micro-organisms in a fluidized bed reactor. *Microbiology* **1996**, *142*, 2187–2196. [CrossRef]
21. American Public Health Association (APHA). *Standard Methods for the Examination of Water and Wastewater*, 21st ed.; APHA: Washington, DC, USA, 2005.
22. Hornbeck, P. Enzyme-linked immunosorbent assays. *Curr. Protoc. Immunol.* **1992**, *1*, 2.1.1–2.1.22. [CrossRef]
23. Ya, T.; Hu, M.; Wang, J.; Zhang, G.; Chen, T.; Duan, L.; Wang, X. Autotrophic biological nitrogen removal in anammox system at elevated temperature: EPS regulation and metagenomic analysis. *Chem. Eng. J.* **2024**, *498*, 155838. [CrossRef]
24. Zhang, S.; Yuan, L.; Li, Y.; Zhao, B. Characterization of ultrafiltration-fractionated humic acid derived from Chinese weathered coal by spectroscopic techniques. *Agronomy* **2021**, *11*, 2030. [CrossRef]
25. Han, K.; Zhang, J.; Wang, C.; Chang, Y.; Zhang, Z.; Xie, J. Alleviative effect of exogenous application of fulvic acid on nitrate stress in spinach (*Spinacia oleracea* L.). *Agronomy* **2024**, *14*, 2280. [CrossRef]
26. Zhao, C.; Liu, H.; Liu, H.; Zhan, X.; Zhang, X.; Fu, B.; Shi, M.; Lu, S.; Huang, F.; Cui, M.; et al. Influence of thermal hydrolysis on sludge anaerobic digestion: Release of humic acid promotes electron transport of methanogen. *Chem. Eng. J.* **2023**, *451*, 138455. [CrossRef]
27. Wen, X.; Zhou, Y.; Liang, X.; Li, J.; Huang, Y.; Li, Q. Impacts of exogenous quorum sensing signal molecule-acylated homoserine lactones (AHLs) with different addition modes on anammox process. *Bioresour. Technol.* **2023**, *371*, 128614. [CrossRef]
28. He, S.; Zhao, L.; Feng, L.; Zhao, W.; Liu, Y.; Hu, T. Mechanistic insight into the aggregation ability of anammox microorganisms: Roles of polarity, composition and molecular structure of extracellular polymeric substances. *Water Res.* **2024**, *254*, 121438. [CrossRef]
29. Zhu, L.; Ma, J.; Wang, Z.; Han, Y.; Chen, L.; Sun, H.; He, Q.; Deng, L.; Shi, Z.; Ke, S. Complete nitrogen removal via novel nitrite-absent anodic anammox process with granular sludge in titanium anode microbial electrolysis cells. *Chem. Eng. J.* **2025**, *493*, 165407. [CrossRef]
30. Hu, P.; van Loosdrecht, M.; Gu, J.-D.; Yang, Y. The core anammox redox reaction system of 12 anammox bacterial genera and their evolution and application implications. *Water Res.* **2025**, *281*, 123551. [CrossRef]
31. Ji, J.; Yang, H.; Li, Y.; Wang, Q.; Dong, Y.; Hu, F.; Wu, G.; Bai, Z.; Chai, F.; Liu, L.; et al. Response of the partial denitrification coupled with anaerobic ammonia oxidation system to disinfectant residues stress. *J. Hazard. Mater.* **2025**, *489*, 137723. [CrossRef]

32. Yang, J.; Huang, D.; Wu, G.; Han, N.; Fan, N.; Jin, R. Quorum sensing-mediated microecological homeostasis in anammox consortia. *J. Hazard. Mater.* **2025**, *492*, 138285. [CrossRef]
33. Wang, X.; Han, N.; Yang, J.; Fan, N.; Jin, R. Metagenomic insight into the diffusion-signal-factor-mediated social traits of anammox consortia after starvation. *J. Environ. Manag.* **2025**, *375*, 124270. [CrossRef]
34. Wang, H.; Xu, H.; Liu, X.; Hua, Y.; Yang, D.; Dai, X. A novel process based on powder carriers demonstrates robustness in nitrogen and phosphorus removal from real municipal wastewater. *Water Res.* **2024**, *251*, 121149. [CrossRef]
35. Wang, H.; Wu, B.; Han, H.; Gu, Q.; Dai, X. Pilot-scale integration of micron-sized powder carriers and a hydrocyclone separator enhances nutrient removal in wastewater treatment. *Commun. Eng.* **2025**, *4*, 158. [CrossRef]
36. Peng, X.; Bao, R.; Xue, L.; Zhou, X.; Ma, X.; Luo, J. Effects of COD on the nitrogen removal pathways and microbial community structure in the anammox system with mixed biofilm-floc sludge. *Process Saf. Environ. Prot.* **2025**, *191*, 107375. [CrossRef]
37. Luo, Q.; Li, Y.; Chang, B.; Zhang, S.; Chen, D.; Jin, R.; Yang, G.-F. Response of biofilm and granular sludge to low dissolved oxygen and organics in a single anammox reactor: Performance, bacterial community and function genes. *J. Environ. Chem. Eng.* **2025**, *13*, 117753. [CrossRef]
38. Zheng, Y.; Shi, L.; Su, R.; Min, W.; Wei, Y.; Ma, B. Effects of periodic starvation on the characteristics and microbial communities of anammox sludge. *J. Environ. Chem. Eng.* **2025**, *13*, 116742. [CrossRef]
39. Wang, R.; Lian, J.; Wang, W.; Shapleigh, J.P.; Jiang, L.; Wang, Y.; Huang, Y.; Xie, L.; Deng, L.; Wang, W.; et al. Metagenomics and metatranscriptomics uncover the regulatory mechanism of nitrogen metabolism response to aggregation status of anammox bacteria. *Chem. Eng. J.* **2025**, *511*, 162179. [CrossRef]
40. Yokota, N.; Mineshima, R.; Watanabe, Y.; Tokutomi, T.; Kiyokawa, T.; Nishiyama, T.; Fujii, T.; Furukawa, K. Startup of pilot-scale single-stage nitrogen removal using anammox and partial nitritation (SNAP) reactor for waste brine treatment using marine anammox bacteria. *J. Biosci. Bioeng.* **2021**, *132*, 505–512. [CrossRef]
41. Wang, D.; Luo, Q.; Huang, K.; Zhang, X. Distinct mechanisms underlying assembly processes and interactions of microbial communities in two single-stage bioreactors coupling anammox with denitrification. *Chem. Eng. J.* **2023**, *452*, 139319. [CrossRef]

Disclaimer/Publisher's Note: The statements, opinions and data contained in all publications are solely those of the individual author(s) and contributor(s) and not of MDPI and/or the editor(s). MDPI and/or the editor(s) disclaim responsibility for any injury to people or property resulting from any ideas, methods, instructions or products referred to in the content.